Thermochimica Acta, 145 (1989) 19–32
Elsevier Science Publishers B.V., Amsterdam – Printed in The Netherlands

STUDY OF COPPER–CHROMIUM OXIDE CATALYST. II*. CRYSTAL DATA AND THERMAL DECOMPOSITION OF BASIC COPPER(II) AMMONIUM CHROMATE

F. HANIC, I. HORVÁTH and G. PLESCH

Institute of Inorganic Chemistry, Centre for Chemical Research, Slovak Academy of Sciences, Dúbravská cesta, 842 36 Bratislava (Czechoslovakia)

(Received July 11 1988)

ABSTRACT

Basic copper(II) ammonium chromate (BCAC) of the composition $CuCrO_4(Cu(OH)_2)_x(NH_4OH)_y(NH_3)_z$ has been prepared. Depending on the pH of the precipitation reaction, quotients x, y and z vary in the intervals $0 < x < 0.3$, $0.6 < y < 0.9$ and $0 < z < 0.2$. The rational formula has been established from the elemental analysis, TG measurements, and from infrared and electronic spectra. The monoclinic unit cell parameters of BCAC were determined by X-ray powder diffraction ($a = 1.0235(15)$ nm, $b = 0.654(2)$ nm, $c = 0.7277(12)$ nm, $\beta = 103.5(1)$ deg, $V = 0.47364$ nm^3, the space group is $C2/m$, Z is 4 and $D_m = (2.98 \pm 0.04)$ Mg m^{-3}). The thermal decomposition of BCAC proceeds in four steps. The activation parameters, E_a, A, $\Delta H^{\neq}$ and $\Delta S^{\neq}$, of the first step of the thermal decomposition were derived.

INTRODUCTION

The starting compound for preparation of the Adkins' copper–chromium oxide catalyst is basic copper(II) ammonium chromate (BCAC). The chemical composition of BCAC was described in earlier studies by the simplified formula $CuCrO_4 \cdot NH_4OH$ [1,2]. It was supposed that the thermal decomposition of BCAC proceeds in two steps [1–3]

$$2CuCrO_4 \cdot NH_4OH \xrightarrow{560\text{–}580\ K} CuO + CuCr_2O_4 + N_2\uparrow + 5H_2O \quad (1)$$

$$CuO + CuCr_2O_4 \xrightarrow[1100\text{–}1170\ K\ in\ air]{1010\text{–}1080\ K\ in\ N_2} 2CuCrO_2 + \tfrac{1}{2}O_2\uparrow \quad (2)$$

However, Patanaik et al. [4] later found that the thermal decomposition of BCAC is a more complex process. According to their data, the decomposition reaction proceeds in three steps and the Cu/Cr ratio in BCAC differs from 1.

* For part I see ref. 6.

0040-6031/89/$03.50

The aim of the present work was to determine the rational formula of BCAC from elemental analysis, and from X-ray, spectroscopic and thermal measurements. It was assumed that the decomposition reactions at higher temperatures, as well as the properties of the products, depend on the chemical composition of BCAC; this information should help to elucidate the high temperature decomposition processes.

EXPERIMENTAL

Sample preparation

BCAC was obtained by the reaction of $CuSO_4 \cdot 5H_2O$ with $(NH_4)_2Cr_2O_7$ in molar ration 2 : 1 i.e. 25 g of $CuSO_4 \cdot 5H_2O$ in 150 ml H_2O was mixed at 330 K with a solution of 12.6 g $(NH_4)_2Cr_2O_7$ in 100 ml H_2O containing varying amounts of aqueous ammonia (27 wt.% NH_3) to obtain an acid, neutral or alkaline pH. The chromatic complex was precipitated in the form of a red-brown sediment. The yield of the reaction and the chemical composition of BCAC varied with pH, see Table 1. The obtained products were dried at 380 K overnight.

The yield of the reaction (Table 1) at pH 3.6 decreased due to the formation of soluble chromates, while at pH 8.5, soluble copper(II) ammine complexes were partially formed. These effects are avoided at pH 7.2.

Methods of investigation

Chemical analysis

The copper and chromium contents in the BCAC samples were determined by atomic absorption spectroscopy (AAS-1 spectrometer, C. Zeiss, Jena), and the nitrogen and hydrogen contents were measured by elemental analysis (Table 4 below).

TABLE 1
Dependence of Cu/Cr, N/Cr and density of BCAC on pH of the precipitation reaction

Aqueous ammonia used in reaction (cm^3 of 27% NH_3)	pH	Cu/Cr	N/Cr	Density (Mg m^{-3})	Yield of reaction (g)
8.5	3.6	1.08	0.78	3.005 ($\pm$0.050)	11.3
17.0	7.2	1.04	0.92	2.985 ($\pm$0.030)	20.5
25.5	8.5	1.14	0.90	3.130 ($\pm$0.050)	13.3

TABLE 2
Crystal data on BCAC synthesized at different pH values

$a = 1.0235(15)$ nm
$b = 0.654(2)$ nm
$c = 0.7277(12)$ nm
$\beta = 103.5(1)$ deg
$V = 0.4736$ nm^3
$Z = 4$
Space group = $C2/m$ or Cm
pH 7.2: $D_m = 2.985$ Mg m^{-3}, MW = 212.9 ± 2.8
pH 3.6: $D_m = 3.005$ Mg m^{-3}, MW = 214.3 ± 3.5
pH 8.5: $D_m = 3.130$ Mg m^{-3}, MW = 223.2 ± 3.6

X-ray methods

The X-ray powder diffraction patterns were taken on a Philips 1540 powder diffractometer using Cu $K\alpha$ radiation. The diffraction data (the

TABLE 3
Observed and calculated d_{hkl} values and relative intensities I_{hkl} of reflections h, k and l of BCAC (pH 7.2); calculations based on crystal data in Table 2

(h k l)	d_{obs} (nm)	d_{cal} (nm)	$(I_{obs})_{rel}$
(0 0 1)	0.7081	0.7076	100
(2 0 0)	0.4969	0.4976	20
(2 0 1)	0.3684	0.3686	72
(0 2 0)	0.3271	0.3270	97
(3 1 0)	0.2955	0.2959	38
(3 1 $\bar{1}$)		0.2957	
(2 2 0)	0.2730	0.2733	36
(2 0 2)	0.2613	0.2610	25
(3 1 $\bar{2}$)	0.2541	0.2545	73
(4 0 $\bar{1}$)		0.2540	
(4 0 0)	0.2488	0.2488	13
(0 0 3)	0.2359	0.2359	16
(4 0 $\bar{2}$)	0.2307	0.2304	37
(1 1 $\bar{3}$)	0.2275	0.2274	15
(2 0 3)	0.1959	0.1962	17
(4 0 2)	0.1842	0.1843	< 5
(3 3 0)	0.1821	0.1822	< 5
(4 2 1)		0.1821	
(0 0 4)	0.1767	0.1769	< 5
(5 1 1)	0.1746	0.1744	< 5
(3 3 1)	0.1710	0.1712	< 5
(3 3 $\bar{2}$)		0.1711	

intensities and interplanar spacings of the reflections) of the BCAC samples agreed with those reported by Stroupe [5]. However, we were able to index the diffraction pattern and to use it for refinement of the unit cell parameters, as well as for determination of the monoclinic space group symmetry. The results are given in Table 2. The indexed powder diffraction data are summarized in Table 3. The d_{cal} values were calculated from the crystal data given in Table 2. The intensities of the X-ray reflections are given on a relative scale.

The products of the high temperature decomposition processes in air were studied on a high temperature Rigaku Denki powder diffractometer with a programmable heating procedure and with a temperature stability ± 1 K during isothermal experiments. The products of the thermal decomposition of BCAC in air or nitrogen atmospheres could also be examined by powder diffraction at room temperature because of the irreversibility of the high temperature decomposition reactions.

Density determination

The densities of the BCAC samples were determined by pycnometry using distilled water for calibration of the pycnometer (the pycnometer volume) and for determination of the sample volumes. It was necessary to remove all air bubbles; this was achieved at reduced pressure. The molecular weight, MW_{BCAC}, was calculated from the unit cell volume V_{BCAC} (Table 2) and the measured density D_m (Table 1) using the formula

$$MW_{BCAC} = AV_{BCAC}D_m/Z \tag{3}$$

where A is Avogadro's number and Z is the number of formula units in the unit cell. The volume V_{BCAC} was found to be equal, within significant deviations (3σ), for all the products synthesized at different pH values.

Thermal methods

Thermal decomposition of BCAC was studied with a DuPont 990 Thermoanalyzer (TGA 951 and DSC cell) in static air and flowing N_2 (1 cm^3 s^{-1}) using 10–15 mg samples and a heating rate of 10 K min^{-1}.

The kinetics of the decomposition of BCAC were studied isothermally using TG in flowing nitrogen and in static air.

Spectral methods

The infrared spectra were measured on a Perkin–Elmer 983 G instrument in the 250–4000 cm^{-1} range, using KBr pellets.

The electronic spectra were measured on a Specord M40 (C. Zeiss, Jena) in the 12000–30000 cm^{-1} range, in Nujol mulls.

RESULTS AND DISCUSSION

Crystallographic and spectral characteristics of BCAC

The IR spectra of BCAC prepared at pH 3.6 and 7.2 are shown in Fig. 1. The presence of (NH_4^+) groups in the compounds is indicated by a strong absorption band υ_4 at 1406 cm^{-1} as well as by a broad band υ_1 at 3240 cm^{-1} with shoulders at 2940 and 2860 cm^{-1}. The presence of OH groups, probably attached to Cu^{2+}, can be correlated with symmetric and antisymmetric vibrations at 3428 and 3304 cm^{-1}. The less intense bands at 1112 and 954 cm^{-1} probably correspond to the bending vibrations of the OH groups. Some of these groups probably participate in bridging bonds of the type Cu–OH–Cu or Cu–OH–Cr.

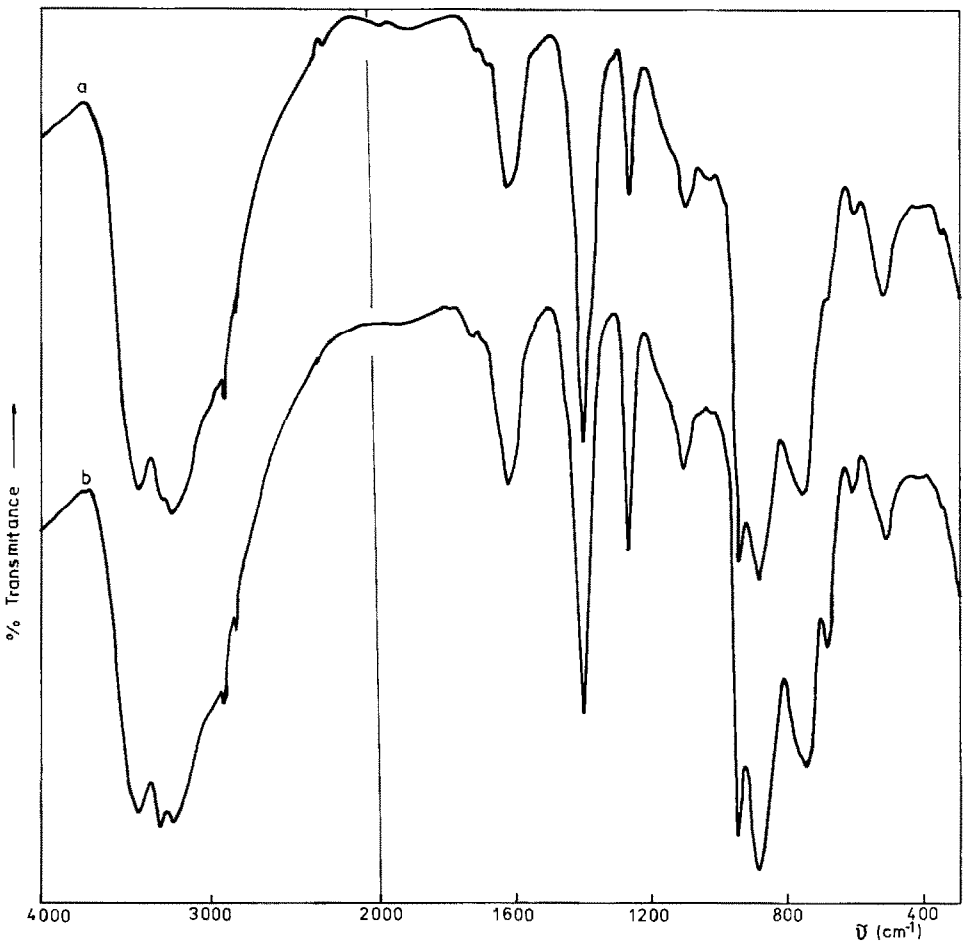

Fig. 1. IR absorption spectra of BCAC: curve a, prepared at pH 3.6; curve b, prepared at pH 7.2.

The strong bands at 895 and 749 cm^{-1} are ascribed to the valence vibrations of the (CrO_4^{2-}) groups.

The absorption band at 1274 cm^{-1} corresponds to NH_3 coordinated to Cu^{2+} in the form $(Cu(NH_3)_n)^{2+}$. It was found that the intensity of this band depends on the pH of the precipitation reaction. The band intensity increases with increasing pH i.e. with increasing amount of ammonia used in the precipitation reaction (Fig. 1). The broad absorption at 1630 cm^{-1} corresponds to the δ_d vibration of NH_3 and NH_4^+.

The absorption band at 516 cm^{-1} represents Cu–O vibration.

Electronic spectra show a broad absorption in the range 22000–30000 cm^{-1} corresponding to the sum of the charge transfer bands oxygen–chromium and oxygen–copper. The maximum of the d–d transition on the Cu^{2+} ion occurs at 13200 cm^{-1} which corresponds to an elongated octahedral coordination of copper ions by oxygen ions in a similar way as occurs in $CuCrO_4$ [6].

The results of the spectroscopic and elemental analysis (Table 4) are consistent with a rational formula of basic copper(II) ammonium chromate

$$\left[(Cu^{2+})_{1+x}(NH_4^+)_y(CrO_4^{2-})(OH^-)_{2x+y}(NH_3)_z\right] \tag{4}$$

where

$$Cu/Cr = a = 1 + x \tag{5}$$

$$N/Cr = b = y + z \tag{6}$$

The values of Cu/Cr and N/Cr are given in Table 1.

The molecular weight MW_{BCAC} is, according to eqns. (4)–(6)

$$MW_{BCAC} = 81.978 + 97.554a + 35.046y + 17.031z \tag{7}$$

The values of MW_{BCAC} for different pH values are known from relation (3), see Table 2. Using eqns. (5)–(7), the known values of MW_{BCAC} (Table 2) and the known values of a and b (Table 1), the quotients y and z can be calculated. They are given in Table 4 and compared with the values derived from the TG measurements.

The most probable mechanism for formation of solid solutions of type (4) is a substitution reaction

$$CuCrO_4 \cdot NH_4OH + x\left(Cu(NH_3)_n^{2+}\right)$$
$$= \left[Cu_{1+x}^{2+}(NH_4^+)_{1-2x}(NH_3)_{nx}(CrO_4^{2-})(OH^-)\right] + 2x(NH_4^+) \tag{8}$$

Reaction (8) proceeds in the aqueous system quite steadily. A product having the composition $CuCrO_4 \cdot NH_4OH$ was never obtained in our numerous experiments. Reaction (8) assumes invariable numbers of Cr^{6+}, O^{2-} and OH^- ions in the equivalent positions of the unit cell. If a portion x of the Cu^{2+} ions of the crystal structure enters into interstitial positions, then the

TABLE 4

Chemical analysis and mass losses Δm_i of the four decomposition steps ($i = 1, 2, 3, 4$) of basic copper(II) ammonium chromate $CuCrO_4(Cu(OH)_2)_x(NH_4OH)_y(NH_3)_z$ prepared at various pH values; TG: thermogravimetric measurements; and XRD: X-ray diffraction data

pH	3.6	7.2	8.5
Chemical analysis:			
%Cu calc. (found)	32.02(31.73)	31.00(31.12)	32.44(32.92)
%Cr calc. (found)	24.26(24.10)	24.39(24.56)	23.29(23.56)
%N calc. (found)	5.10 (5.06)	6.05 (6.08)	5.65 (5.74)
%H calc. (found)	1.89 (1.97)	2.08 (1.94)	2.09 (1.85)
	63.27(62.86)	63.52(63.70)	63.47(64.07)
Mass losses in nitrogen:			
Δm_1 calc. (found)	21.0(21.1)	22.2(22.2)	22.0(21.8)
Δm_2 calc. (found)	2.7 (2.0)	2.5 (1.6)	1.9 (1.6)
Δm_3 calc. (found)	0.7 (5.6)	0.3 (5.2)	1.1 (4.3)
Δm_4 calc. (found)	4.0 (0.2)	3.9 (0.1)	4.1 (0.5)
	28.4(28.9)	28.9(29.1)	29.1(28.2)
Mass losses in air:			
Δm_1 calc. (found)	21.0(20.2)	22.2(21.0)	22.0(21.6)
Δm_2 calc. (found)	2.7 (2.8)	2.5 (2.3)	1.9 (2.7)
Δm_3 calc. (found)	0.7 (2.3)	0.3 (0.8)	1.1 (0.7)
Δm_4 calc. (found)	4.0 (4.7)	3.9 (4.3)	4.1 (3.6)
	28.4(30.0)	28.9(28.4)	29.1(28.6)
Formula quotients:			
x	0.08	0.04	0.14
y_{TG} (y_{XRD})	0.76(0.76)	0.78(0.77)	0.82(0.82)
z_{Tg} (z_{XRD})	0.02(0.02)	0.14(0.15)	0.08(0.08)

occupation of the 4-fold equivalent positions by copper ions also remains constant. We believe that some of the equivalent positions of the NH_4^+ ions in the structure of BCAC can be occupied by neutral NH_3 groups from ($Cu(NH_3)_n^{2+}$). Direct evidence of such a substitution can be found when NH_3 gas interacts with the solid solution (BCAC) and the results are examined by IR [7]. The absorption bands corresponding to the NH_3 groups progressively increase, while those of the NH_4^+ and OH^- groups decrease, with increased time of interaction. The intensities of the remaining absorption bands stay unchanged. At the same time, the red-brown colour of the powder changes to green. These observations support the substitutional type of reaction instead of an additional one.

The parameters x and n in reaction (8) are sensitive to pH. It follows, from a comparison of eqns. (4) and (8), that $z \simeq nx$. The number n of NH_3 groups attached to Cu^{2+} can therefore be evaluated from the values of x and z given in Table 4. The n value equals approximately 4 for pH 7.2 and it decreases to a value less than 1 for pH 3.6 and 8.5, respectively.

Thermal decomposition of BCAC

The rational formula (4) predetermines the thermal behaviour of BCAC. The following decomposition processes can be expected: desorption of NH_3; reduction of Cr^{6+} to Cr^{3+} and oxidation of NH_4^+ to N_2 and H_2O; dehydroxylation of the complex; and reduction of Cu^{2+} to Cu^+.

The results of the TG analysis revealed four distinct steps of the thermal decomposition of BCAC both in nitrogen and in static air (Figs. 2 and 3).

The largest amount of volatile compounds (21–22 wt.%) is released in the first step of decomposition in the temperature range 420–625 K. According to the DSC results (Fig. 4), the decomposition starts with the endothermic desorption of ammonia followed by an exothermic autocatalytic oxidation–reduction process, in which the NH_4OH constituent of the chromate complex is oxidized by the $CuCrO_4$ component with evolution of N_2(g) and H_2O(g)

$$2\left[(Cu^{2+})_{1+x}(NH_4^+)_y(CrO_4^{2-})(OH^-)_{2x+y}(NH_3)_z\right]$$
$$= 2(1-y)CuCrO_4 + y(CuO + CuCr_2O_4) + 2xCu(OH)_2 + yN_2\uparrow$$
$$+ 5yH_2O\uparrow + zNH_3\uparrow \qquad (9)$$

The product of the thermal decomposition is a highly disordered system [8] unless the temperature does not rise over the recrystallization temperature

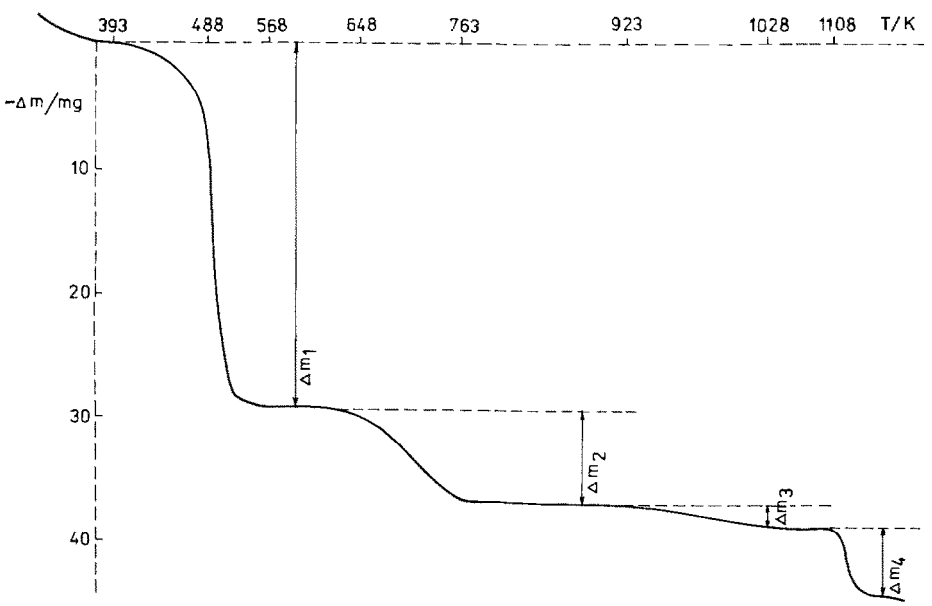

Fig. 2. Typical TG curve of thermal decomposition of BCAC in air (Derivatograph Q 1500, heating rate 10 K min^{-1} using 150 mg sample).

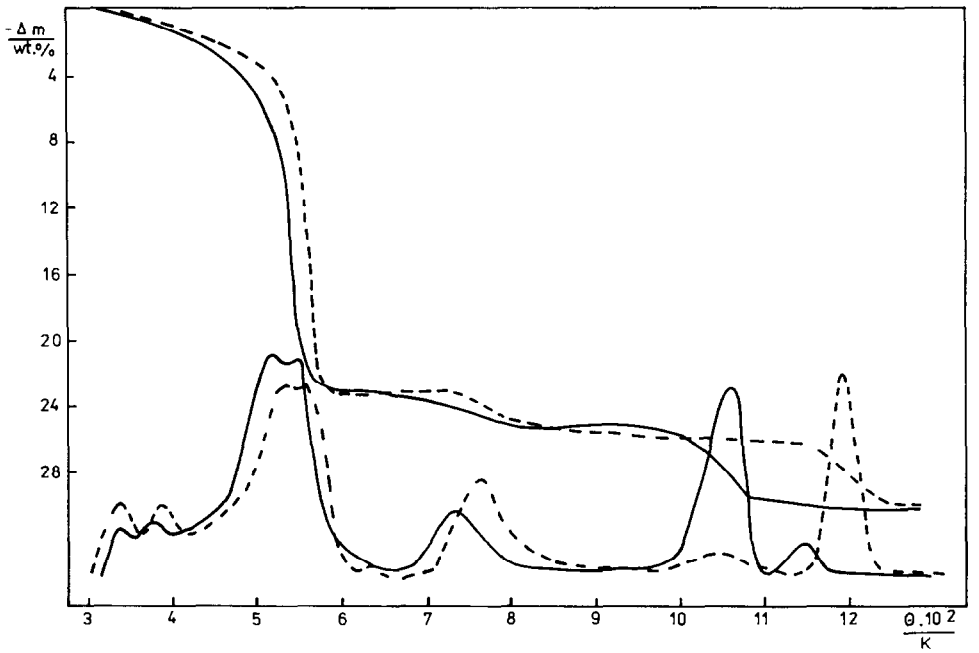

Fig. 3. TG and DTG curves for thermal decomposition of BCAC (Thermoanalyzer DuPont 990): full line, flowing nitrogen; broken line, static air.

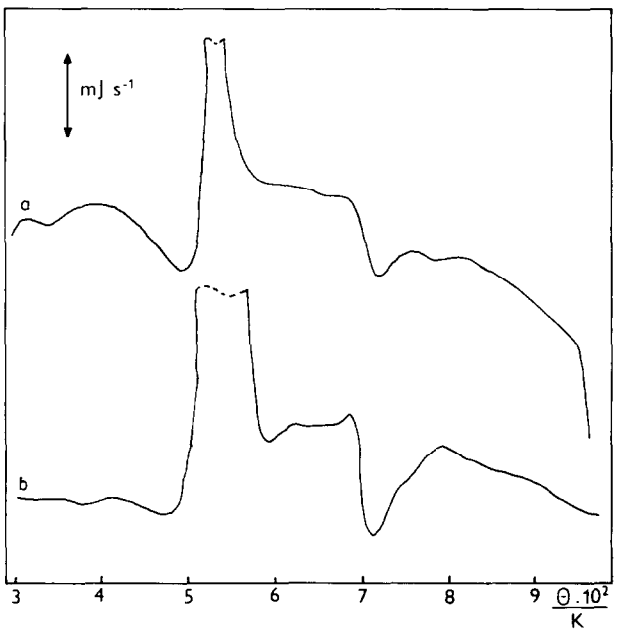

Fig. 4. DSC curve for thermal decomposition of BCAC: curve a, in flowing nitrogen; curve b, in static air.

which is approximately 700 K, according to the DSC measurements. In the recrystallized samples, crystalline CuO and $CuCr_2O_4$ could be detected by X-ray powder diffraction [8]. In some samples, traces of unreacted $CuCrO_4$ could also be identified.

The recrystallization process is involved in the second step of the thermal decomposition of BCAC, in which the endothermic decomposition of the unreacted portion of the $CuCrO_4$ component occurs with formation of CuO and $CuCr_2O_4$ and evolution of O_2(g). This takes place within the range 670–920 K, depending on the atmosphere (Fig. 3). The lower temperature interval is observed in the nitrogen atmosphere.

The release of water (0.7–2.3 wt.%) in the third step of decomposition of BCAC corresponds to a dehydroxylation of the $Cu(OH)_2$ constituent at 920–1120 K in air, according to the scheme

$$CuO + CuCr_2O_4 + 2xCu(OH)_2 = (1 + 2x)CuO + CuCr_2O_4 + 2xH_2O \quad (10)$$

The fourth and the last step of BCAC thermal decomposition represents the reduction of Cu^{2+} to Cu^+ with release of oxygen according to the scheme

$$(1 + 2x)CuO + CuCr_2O_4 = 2CuCrO_2 + xCu_2O + \tfrac{1}{2}(1 + x)O_2 \uparrow \quad (11)$$

The position of the DTG peaks on the temperature scale (Fig. 3) demonstrates the sensitivity of this reaction step to the oxygen partial pressure. The bifurcation of the peak in flowing nitrogen indicates that reaction (11) proceeds in two steps. The low temperature part overlaps with the dehydroxylation reaction, the high temperature part shows a mass loss of 0.1–0.5 wt.% (Table 4). Reduction of Cu^{2+} to Cu^+ in static air proceeds mostly in the range 1120–1240 K. The reason for the existence of different decomposition temperatures of BCAC lies, according to reaction scheme (11), in the different thermal stabilities of CuO and $CuCr_2O_4$ at high temperatures in different atmospheres. Crystalline $CuCrO_2$ was identified as a product of the thermal decomposition using X-ray diffraction methods.

Table 4 summarizes the results of the chemical and thermal analyses. The experimental data (mass % of Cu, Cr, N and H, and the mass losses of Δm_i for the four decomposition steps) are compared with the calculated values. The coefficients x, y and z, necessary for estimation of the theoretical values, were obtained from the crystal data, the density measurements and the chemical analysis using eqns. (3)–(7), and also by determining the values of chosen parameters which reproduce the best fit between the observed and calculated values of Δm_i and of wt.% Cu, Cr, N and H.

Kinetics and mechanism of the first step in the thermal decomposition of BCAC

The most important thermal decomposition reaction of BCAC, from the point of view of its catalytic activity, is the first oxidation–reduction step, in

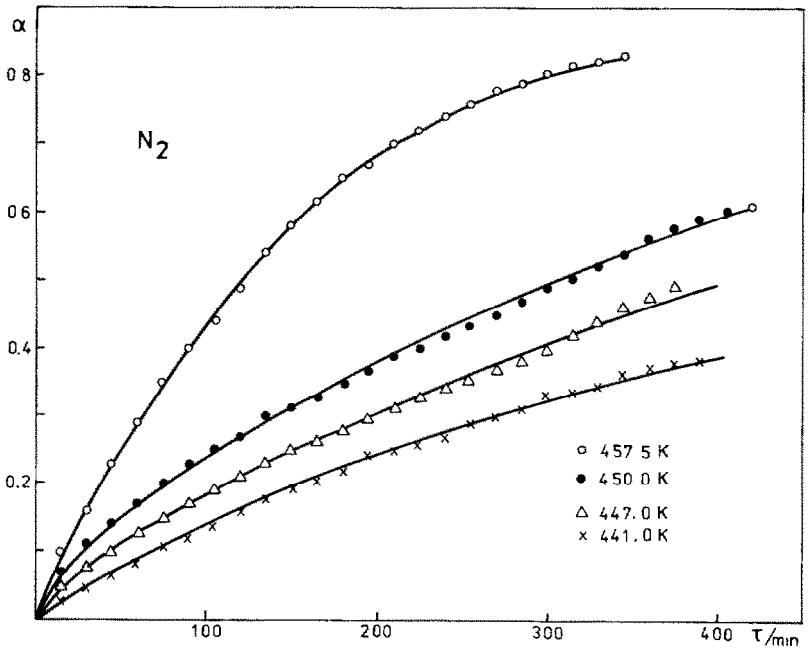

Fig. 5. Isothermal conversions $\alpha = f(t)$ of desorption reaction of ammonia from BCAC in nitrogen expressed as relative TG mass losses at different temperatures.

which ammonia is released and oxidation–reduction processes occur according to scheme (9). The catalysts with the highest activity and selectivity were obtained when BCAC was heated in air within the temperature range 540–570 K for 1 h [8]. With these conditions, the solid products exhibited a highly disordered structure.

The rate of release of gaseous products in the first step of the decomposition reaction was measured by isothermal TG in a nitrogen flow (1 $cm^3\ s^{-1}$) at temperatures lower than the threshold temperature of the autocatalytic reaction (< 520 K). At these temperatures, the endothermic desorption of ammonia and the formation of a highly disordered arrangement have a predominant effect over the exothermic oxidation–reduction process.

The isothermal plots of $\alpha = f(t)$ are shown in Fig. 5. It was found that they obey first-order kinetics up to 75% conversion. This follows from the linear plots of $[-\ln(1-\alpha)]$ against t in Fig. 6, from which the rate constants k_T could be evaluated [9].

The values of the apparent activation energy E_a and the pre-exponential term A were calculated using the Arrhenius relation. Enthalpy and entropy changes of activation, ΔH^* and ΔS^* were determined using the equation

$$\ln(k_T h/kT) = -\Delta H^*/RT + \Delta S^*/R \qquad (12)$$

where k_T is the rate constant at temperature T, and h and k are Planck's

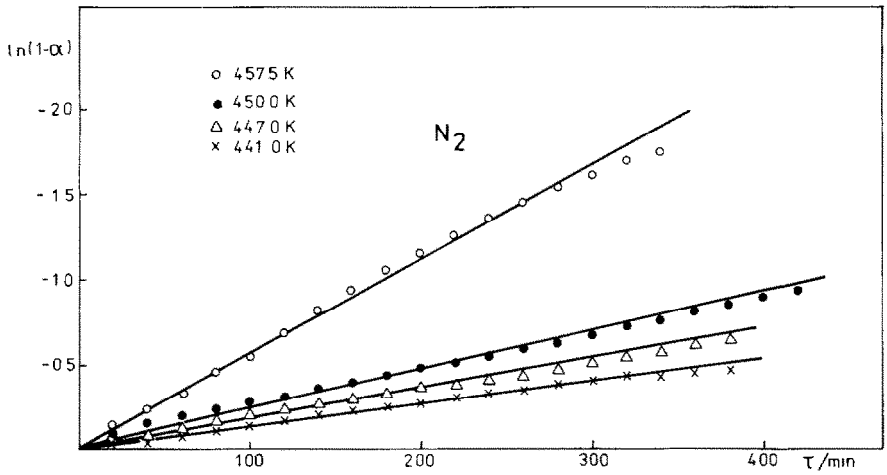

Fig. 6. Fitting of the isothermal desorption TG patterns in nitrogen.

and Boltzmann's constants, respectively. The activation parameters are: $E_a = 145$ kJ mol^{-1}; $A = 3.10^{12}$ s^{-1} with a correlation of 0.978; $\Delta H^{\neq} = 143$ kJ mol^{-1}, $\Delta S^{\neq} = 47$ J K^{-1} mol^{-1}.

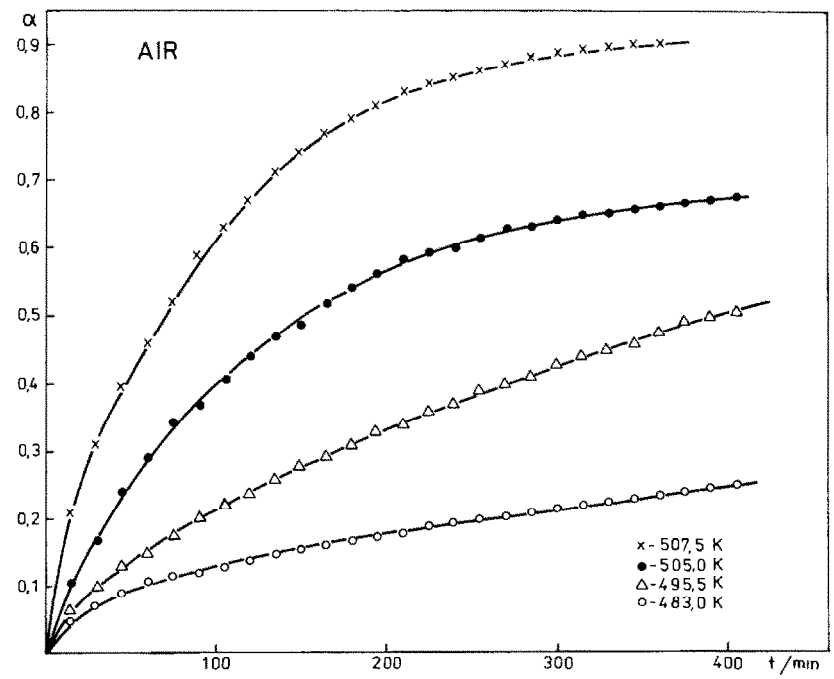

Fig. 7. Isothermal conversions $\alpha = f(t)$ of desorption reaction of ammonia in air expressed as relative TG mass losses at different temperatures.

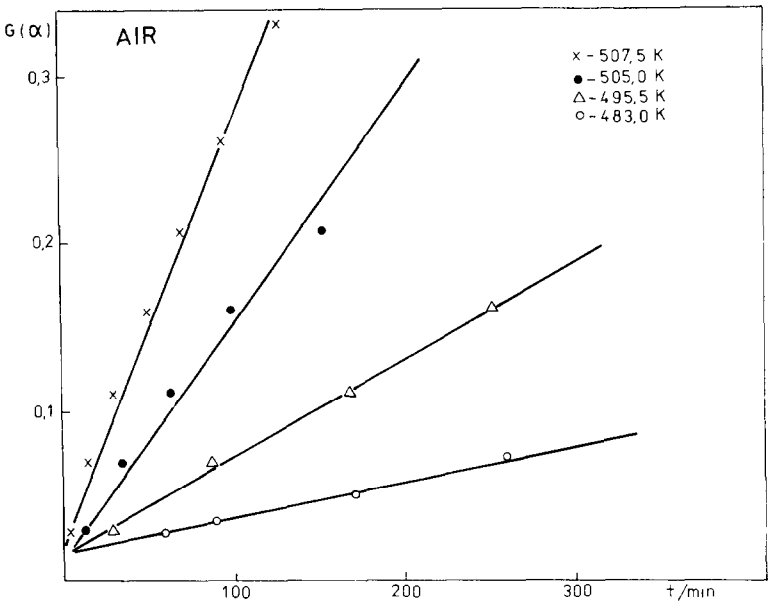

Fig. 8. Fitting of the isothermal TG patterns of ammonia desorption in air.

Conversion in static air (Fig. 7) is consistent within the interval $0.08 < \alpha < 0.40$ with the contraction volume mechanism described by the rate eqn.

$$1 - (1 - \alpha)^{1/3} = k_T t \tag{13}$$

as is demonstrated by the linear dependence of $[1 - (1 - \alpha)^{1/3}]$ versus t (Fig. 8). The activation parameters calculated from the Arrhenius plot and equation (13) are: $E_a = 202$ kJ mol^{-1}; $A = 2.10^{16}$ s^{-1} with a correlation of 0.992; $\Delta H^{\neq} = 198$ kJ mol^{-1}; and $\Delta S^{\neq} = 90$ J K^{-1} mol^{-1}.

CONCLUSIONS

The rational formula of BCAC has been derived, $(Cu^{2+})_{1+x}(NH_4^+)_y$-$(CrO_4^{2-})(OH^-)_{2x+y}(NH_3)_z$, in which the quotients x, y and z depend on the pH of the precipitation reaction. The crystal data of monoclinic BCAC were also derived.

The thermal decomposition of BCAC proceeds in four steps according to the scheme

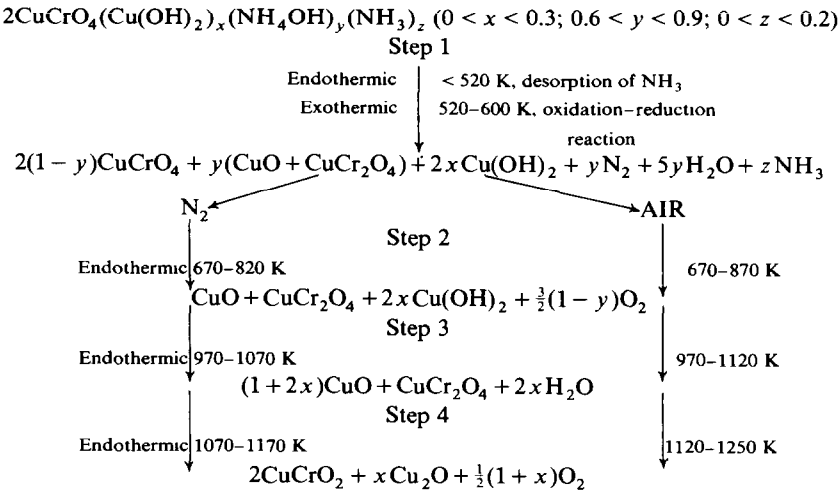

The kinetics and mechanism of Step 1 of the thermal decomposition of BCAC, in nitrogen flow and in static air, have been established from TG isothermal measurements. The activation parameters E_a, A, $\Delta H^{\neq}$ and $\Delta S^{\neq}$ were found.

ACKNOWLEDGEMENT

Critical reading of the manuscript and its communication to the publisher by Dr. Jaroslav Šesták (Institute of Physics, Prague) is gratefully acknowledged.

REFERENCES

1 H. Adkins and R. Connor, J. Am. Chem. Soc., 53 (1931) 1091.
2 M. Stammler and M. Pyzyna, Adv. X-ray Anal., 7 (1964) 229.
3 L. Walter-Levy and M. Goreaud, Bull. Soc. Chim. Fr., (1973) 830.
4 P. Patanaik, D.Y. Rao, P. Ganguli and R.S. Murthy, Thermochim. Acta, 68 (1983) 17.
5 J.D. Stroupe, J. Am. Chem. Soc., 71 (1949) 569.
6 F. Hanic, I. Horváth, G. Plesch and L. Gáliková, J. Solid State Chem., 59 (1985) 190.
7 K. Putyera, G. Plesch and F. Hanic, unpublished results.
8 F. Hanic, G. Plesch, L. Doležel and J. Ovečková, React. Kinet. Catal. Lett., 32 (1986) 393.
9 J. Šesták, Thermophysical Properties of Solids; Their Measurements and Theoretical Thermal Analysis, Academia/Elsevier, Praha/Amsterdam, 1984.